ARTICLE

Femtosecond Four-Wave-Mixing Spectroscopy of Suspended Individual Semiconducting Single-Walled Carbon Nanotubes

Pasi Myllyperkiö,[†] Olli Herranen,[‡] Jyri Rintala,[†] Hua Jiang,[§] Prasantha R. Mudimela,[§] Zhen Zhu,[§] Albert G. Nasibulin,[§] Andreas Johansson,[‡,*] Esko I. Kauppinen,[§] Markus Ahlskog,[‡] and Mika Pettersson[†,*]

[†]Department of Chemistry, [‡]Department of Physics, Nanoscience Center, P.O. Box 35, FI-40014, University of Jyväskylä, Finland, and [§]Department of Applied Physics and Center for New Materials, Aalto University, Puumiehenkuja 2, 00076, Aalto, Finland

ABSTRACT Femtosecond four-wave-mixing (FWM) experiments of individual suspended semiconducting single-walled carbon nanotubes (SWCNTs) are presented. The chiral indices of the tubes were determined by electron diffraction as (28,14) and (24,14) having diameters of 2.90 and 2.61 nm, respectively. The diameter and semiconducting character of the tubes were additionally confirmed by resonance Raman measurements. The FWM signal showed electronic response from the SWCNTs. The results demonstrate that ultrafast dynamics of individual SWCNTs can be studied by FWM spectroscopies.

KEYWORDS: carbon nanotube · four-wave-mixing · electron diffraction · femtosecond · Raman

Optical spectroscopy of nanoobjects poses challenges for experimentalists and theoreticians, alike. One of the fundamental reasons for interest in nanomaterials is the variation in their properties as a function of size and structure of the particle. The major difference from the more traditional materials is that in nanoworld it is important to consider the properties of each individual particle. A striking demonstration of this is provided by the SERS (surface-enhanced Raman scattering) effect which is highly specific for certain structures.[1] Experimental studies of nanoobjects are hampered by the fact that usually it is difficult to obtain pure homodisperse samples of particles with a well-defined structure. From the spectroscopic point of view, this means that one has either to measure average properties of ensembles or to perform measurements of individual particles. Optical spectroscopy of individual nanoparticles is experimentally very challenging, especially for time-resolved measurements. However, for carbon nanotubes (CNT) single-tube Raman spectroscopy is nowadays routinely performed.[2] In addition, emission spectroscopy from ensembles of single-walled CNTs (SWCNT) can be used to characterize the distribution of various tube types in the sample.[3] Spectroscopic analysis of SWCNTs at the level of individual nanotubes is thus important since the electronic properties of SWCNTs vary strongly according to the structure of the tube.[4] Rayleigh scattering has been used to measure electronic absorption spectra of individual suspended SWCNTs and combined with the structure determination by electron diffraction.[5,6]

While the above-mentioned techniques can be used to study electronic and vibrational properties of individual SWCNTs, they give information on the dynamics indirectly, *via* band widths. As far as we know, all of the time-domain (femtosecond) spectroscopic studies of SWCNTs have been conducted on ensembles that yield highly averaged information.[7−9] More specific investigations include pump and probe studies of a sample of (6,5) SWCNTs and studies of SWCNTs by photon echo techniques that eliminate inhomogeneous broadening.[10,11] While these techniques yield valuable insight into the photophysical properties of SWCNTs it would be highly desirable to perform femtosecond dynamics studies of individual SWCNTs. To this end, four-wave-mixing (FWM) with its many variants is a promising technique as it provides a strong signal with a zero-background, and it can be applied to study both vibrational and electronic dynamics. Recently, picosecond FWM imaging of metallic CNTs was demonstrated.[12] However, the time-resolution of the used technique was not sufficient to

*Address correspondence to mika.j.pettersson@jyu.fi, andreas.johansson@jyu.fi.

Received for review July 2, 2010 and accepted October 01, 2010.

Published online October 12, 2010. 10.1021/nn1015067

yield dynamical information. In this work, we extend the FWM technique to the femtosecond regime, which opens the door to direct dynamics studies of individual SWCNTs. To be sure that the measurements are performed on individual SWCNTs, the nanotubes are suspended over a slit and their structure is determined by means of Raman spectroscopy and transmission electron microscopy techniques.

RESULTS AND DISCUSSION

The sample configuration is shown schematically in Figure 1a. The sample geometry allows performing electron diffraction measurements for the tubes and additionally it offers an optimal platform for optical measurements. The slit configuration makes it possible to pinpoint the laser beams accurately to the nanotube location and the scattering of the laser beams from the substrate is eliminated, which is beneficial for measuring very weak signals. Scanning electron micrographs of the actual samples can be viewed in Figure 1b,c. Both samples contain an individual suspended SWCNT, and sample 2 contains additionally a carbon fiber, aligned perpendicular to the nanotube.

Figure 2 presents TEM images (a and d) and corresponding electron diffraction (ED) patterns (b and e) of the two individual SWCNT samples 1 and 2, respectively. The circles in the TEM images indicate the location on each nanotube where the electron diffraction patterns were taken. By using a method based on intrinsic layer line distance analysis,[13] the diffraction patterns (b and e) have been indexed and the chiral indices were determined to be (28, 14) for tube 1 and (24, 14) for tube 2 with the diameters 2.90 and 2.61 nm, respectively. The determined indices identify both tubes as semiconducting ($n - m$ not evenly divisible by 3).

To obtain information on the resonant energy levels of the tubes and thus to help design FWM experiments, Raman measurements on the suspended tubes were performed for both suspended tubes and additionally for an additional tube found on the Si_3N_4 membrane. The spectra of the suspended tubes are shown in Figure 2,c,f. In both cases, the shape of the G band suggests[14] that the tube is semiconducting in agreement with the structures determined by electron diffraction. A single strong and narrow RBM peak also points to a single tube. The small sidebands around the RBM originate from rotational Raman signal of air. Tube 2 has a relatively strong D-band and a shoulder on the blue side of the G-band. It is worth noting that signal from amorphous carbon was detected on top of the Si_3N_4 membrane. Since the slit is relatively narrow with respect to the measurement spot, it is possible that the higher intensity of the D-band and the G-band shoulder for tube 2 contain contribution from amorphous carbon on the surface of the membrane or from the carbon nanofiber visible in the TEM image (2d).

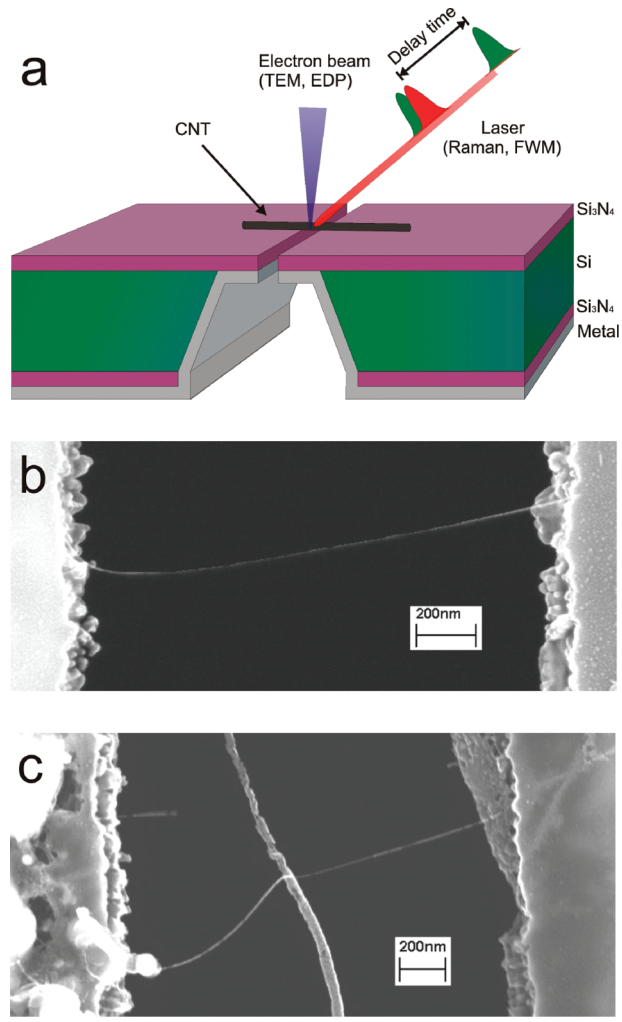

Figure 1. (a) Schematic of the sample layout; (b) scanning electron micrograph of a CNT suspended freely across the slit (sample 1); (c) scanning electron micrograph of a suspended CNT (sample 2), which is supported at its midpoint by a carbon fiber.

Using the relation between the frequency of the RBM mode (ω_{RBM}) and the diameter (d) of the tube, $d = 227.0/\omega_{RBM}$, obtained for a large number of long isolated SWCNTs grown by the "supergrowth" method,[15] we get another evaluation of the tube diameters. The frequency of the RBM mode for tube 1 is 75.8 cm^{-1} and the frequency for tube 2 is 90.1 cm^{-1} giving a diameter of 2.99 and 2.52 nm, respectively. These values are in good agreement with those obtained from the electron diffraction analysis. On the other hand, using the relation $d = 204/(\omega_{RBM} - 27)$, which was obtained for suspended SWCNTs[16−18] leads to a severe overestimate of the diameters (4.2 and 3.2 nm). This discrepancy shows that still more work is needed to fully understand the different factors that affect the relation between the diameter and the frequency of RBM. A spectrum of one more tube lying on the membrane was also measured (not shown) which indicated that the tube is individual, semiconducting, 2.0 nm in diameter, and it has a low intensity of the D-band.

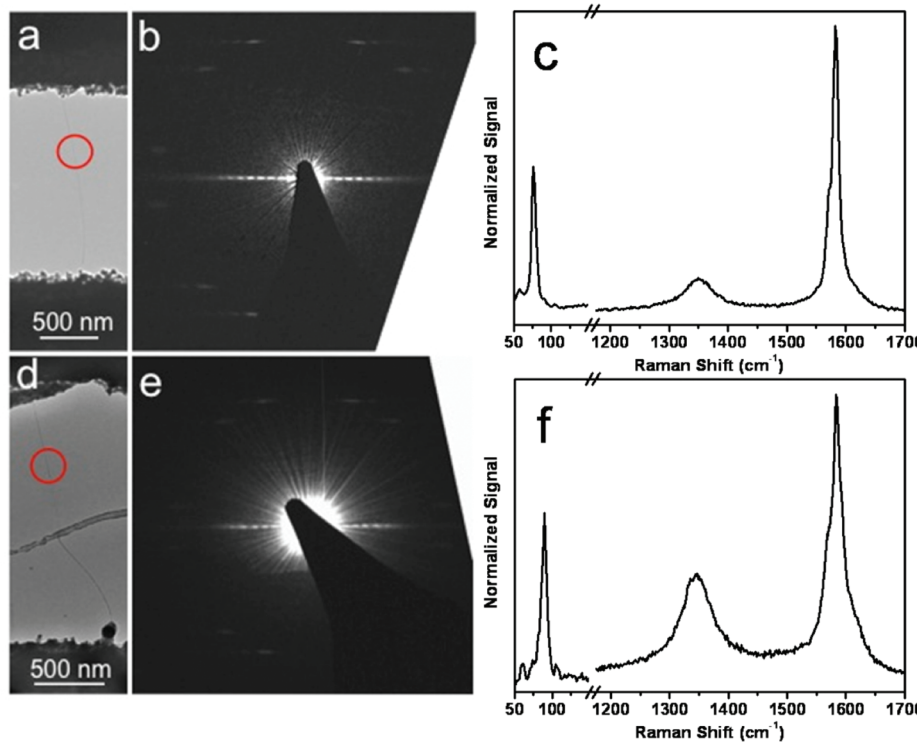

Figure 2. (a and d) TEM images of samples 1 and 2, respectively; (b and e) the corresponding ED patterns taken at the encircled locations; (c and f) Raman spectra measured from the suspended SWCNTs.

The femtosecond experiments were designed to perform FWM on suspended SWCNTs. FWM is a general name for a family of nonlinear electronic and vibrational spectroscopies that employ three input electromagnetic fields that are mixed in the material of interest yielding a fourth signal field that is detected. The signal field is emitted by the third order polarization which is a result of a convolution of the excitation fields (E) with the material response function.[19]

$$P^{(3)}(\vec{r},t) = \int_0^\infty \int_0^\infty \int_0^\infty dt_3 dt_2 dt_1\, S^{(3)}(t_3,t_2,t_1)\, E(\vec{r},t-t_3) \times E(\vec{r},t-t_3-t_2)\, E(\vec{r},t-t_3-t_2-t_1) \quad (1)$$

The response function $S^{(3)}(t_3, t_2, t_1)$ carries all the information of the system, and the experimental challenge is to design the input fields in such a way that useful information is obtained. Depending on the specific technique either electronic or vibrational dynamics is probed. Well-known examples of FWM techniques include coherent anti-Stokes Raman scattering (CARS), photon echo, and transient grating. Experimental control over what dynamics is probed depends on timing of the pulses and the direction and wavelength of the measured signal. For microscopic applications that require the use of tight focusing with objectives with high numerical aperture (NA) collinear input beams must be used which eliminates the possibility to choose the direction of the signal. On the other hand, tight focusing relaxes the phase-matching condition as demonstrated in CARS microscopy.[20]

The experiment was performed by overlapping temporally the pump and Stokes pulses and varying the probe pulse time delay while simultaneously detecting the signal at the anti-Stokes frequency ($\omega = \omega_{pump} - \omega_{Stokes} + \omega_{probe}$). A fundamental problem in using two colors and a collinear beam geometry is that the signal originating from double interaction with the pump ($\omega = 2\omega_{pump} - \omega_{Stokes}$) cannot be distinguished from the signal originating from the interaction of pump and probe beams ($\omega = \omega_{pump} - \omega_{Stokes} + \omega_{probe}$). This introduces a constant background signal which obviously does not depend on the time delay between the Stokes and probe pulses. To improve the situation, for sample 2, the probe beam was chopped at 500 Hz, and the signal was recorded using a lock-in-amplifier.

The pump excitation wavelength was tuned to 532 nm based on the Raman measurements that indicated resonance at this wavelength. The energy diagram of the FWM measurement is shown in Figure 3. The measured spectra of the pump (as well as probe), Stokes, and signal beams are shown in the lower panel. For thick tubes, several electronic resonances, denoted E_{nn} ($n = 1, 2, 3, ...$) are expected to lie in the relevant spectral region. As there is no experimental data available for higher transitions of thick tubes, we estimated these resonances using empirical relations.[21,22] The accuracy of this approach was checked against transition energies determined by Rayleigh scattering for several suspended tubes.[5] For a set of eight semiconducting tubes varying in diameter between 1.63 and 1.84 nm, the model gives the energies of the E_{33} and E_{44} transitions

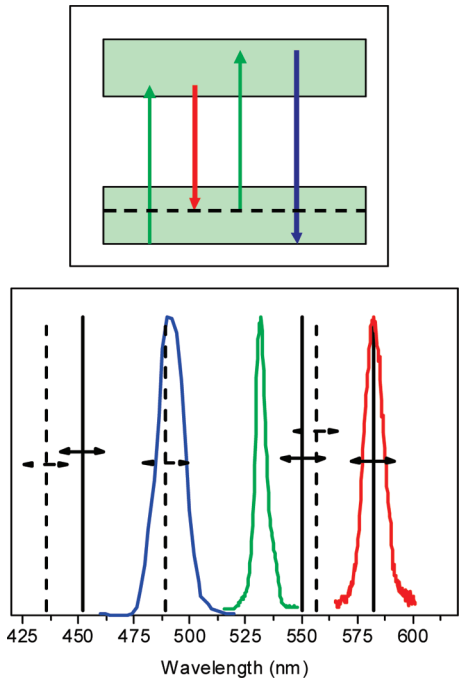

Figure 3. Lower panel: experimental spectra of pump and probe (green), Stokes (red), and signal (blue) beams used in the FWM experiment. The solid lines indicate estimated (following refs 21, 22) transition energies corresponding with the E_{55}, E_{66}, and E_{77} transitions (from right to left) of the 28,14 tube (sample 1) and the dashed lines indicate the corresponding transition energies of the 24,14 tube (sample 2). The double-headed arrows indicate the estimated half-width of the transitions. Upper panel: a scheme indicating the four interactions of the system with electromagnetic fields. The colors correspond to those in the lower panel.

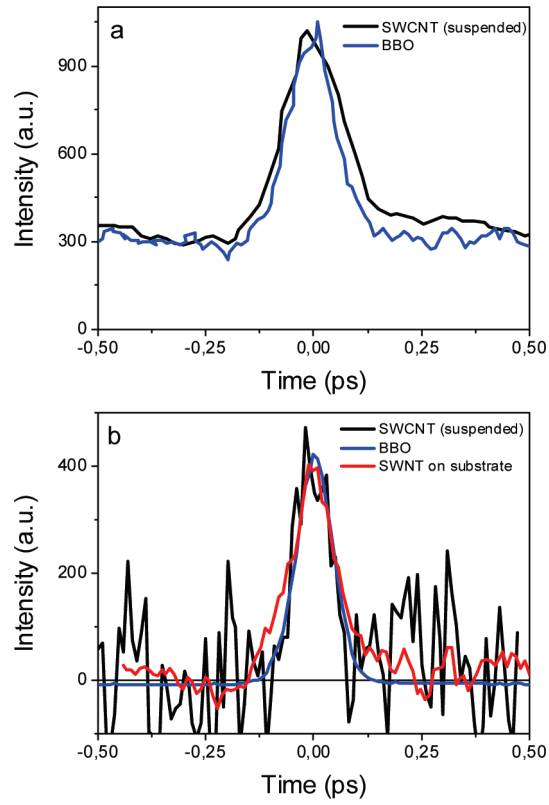

Figure 4. Femtosecond FWM signal of suspended SWCNTs in (a) sample 1 and (b) sample 2. The signal is measured as a function of the time delay between the Stokes and probe pulses: (black line) SWCNT; (blue line) reference signal from BBO; (red line) SWCNT on Si_3N_4 membrane.

with an average deviation of 0.024 meV. Although in this work higher transitions are probed (E_{55}, E_{66}), we believe that the predictions of the model are still useful. In Figure 3, solid lines indicate the positions of estimated transition energies for tube 1 and the corresponding transitions for tube 2 are denoted with dashed lines. The widths of the transitions are estimated to be ~100 meV based on the measured widths of 80−90 meV for suspended nanotubes for E_{33} and E_{44} transitions.[6] This corresponds to ~20 nm width in the spectral region of interest, and it is marked in Figure 3 with double-headed arrows. The upper panel of Figure 3 indicates the interactions of the system with electromagnetic fields in the FWM process. Several interactions can be in electronic resonance with the nanotube which leads to enhancement of the signal. In particular, according to Figure 3, the Stokes transition is in resonance with tube 1 and the FWM signal is in resonance with tube 2. The pump is weakly in resonance within the bandwidth for both tubes, tube 1 being closer to the resonance. In addition, the Stokes shift was adjusted to be in vibrational resonance with the Raman transition of the G-band. The bandwidth of the femtosecond pulses matches very well with the bandwidth of the electronic transitions which is favorable for maximizing the excitation efficiency.

Before presenting the results of the current work we briefly review the previous picosecond FWM results by Kim *et al.*[12] They observed signal only from metallic nanotubes which was attributed to lower polarizability of semiconducting tubes. They investigated the nature of FWM response of multiwalled CNTs and found that it is mainly electronic in nature while vibrational response was additionally detected from graphitic clusters. The diameter of their tubes lying on a quartz substrate was determined by AFM measurements. It can be argued that the accuracy is probably not enough to distinguish reliably between SWCNTs or small MWNTs or small bundles. Thus, some uncertainty remains in the actual identity of the measured samples.

Whereas in ref 12, the FWM experiment was carried out with spectrally narrow and temporally long pulses, we use temporally short femtosecond pulses to investigate the dynamics of SWCNTs. The main results of this study are shown in Figure 4 where the homodyne-detected FWM signal as a function of the delay between the Stokes and probe pulses is shown for both suspended tubes. The signals for tubes 1 and 2 are shown in panels a and b, respectively. In panel a the signal is relatively strong and it is localized around the zero delay where all electronic, vibrational, and nonresonant effects contribute to $P^{(3)}(t)$. The offset in the signal is due to two-pulse contribution which does not de-

pend on the delay between pulses. Importantly, the ED and resonance Raman measurements confirm that the measured tubes are semiconducting and that they are individual. Thus, our results demonstrate the first example of FWM of individual semiconducting tubes.

The FWM signal, measured in forward geometry from a 100 μm thick BBO crystal, carefully placed in focus as in the SWCNT measurement, is shown in Figure 4 with a blue line. The BBO-result gives essentially the convolution of the three pulses, whereas the signal measured from the nanotube contains additionally the response of the system which appears to be broadened compared to the BBO-reference. The BBO-signal was measured before and after the SWCNT measurement with consistent results. The system response includes electronic (excitonic) and vibrational coherence and the electronic response may in principle contain several processes corresponding to different time-ordering of the interacting fields.[19] The measured signal can be safely assigned predominantly to the electronic response since the vibrational coherence should be much longer. On the basis of the Raman linewidths of individual SWCNTs and time-resolved CARS measurements of the G-band from SWCNT ensembles, vibrational coherence should be visible as a decay with a time constant of about 1 ps.[8,9] There is slightly increased signal level also at positive times but it cannot be reliably assigned to a real signal attributable to vibrational coherence. Since the specific processes contributing to the signal cannot be singled out we simply suffice to model the situation with a convolution of three pulses with an exponentially decaying average system response (electronic dephasing). In the simulation, the pump and Stokes pulses are temporally overlapped while the probe pulse is swept in time. This analysis yields a dephasing time of 45 fs. Taking into account the approximations and quality of the data this result should be treated as a rough estimate. Nevertheless, it seems reasonable when comparing it with values from literature. Rayleigh scattering measurements of suspended SWCNTs yielded linewidths between 10 and 90 meV depending on the transition. For higher E_{33} and E_{44} transitions, which are closer to our situation, the width of 80−90 meV was observed.[6] This corresponds to a dephasing time of ~15 fs. Photon echo measurements of SWCNT ensembles revealed a pure exciton dephasing time of 78 fs for E_{11} transitions.[11] In this respect our value seems reasonable, but further experiments are needed to make more quantitative analysis.

The data for tube 2 in panel b shows that the signal is much weaker but still reliably detectable. This could be due to less favorable resonance conditions for this tube. A much stronger signal was found outside the slit, on the membrane, and it is shown in panel b with a red line. On the basis of the approximate position of the species producing the signal, we measured the resonance Raman spectrum from

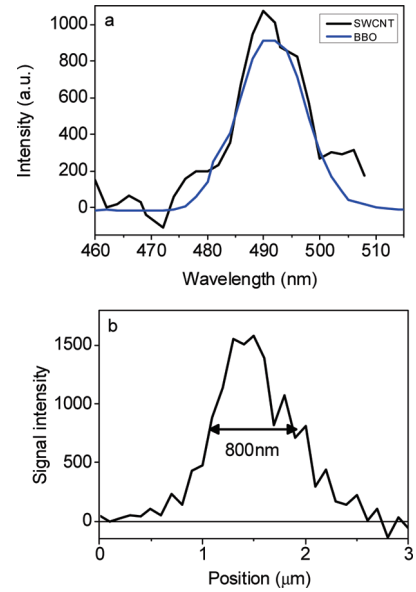

Figure 5. (a) Spectrum of the FWM signal from BBO (blue line) and from a SWCNT on top of the Si_3N_4 membrane (black line). (b) Scan of the FWM signal over a SWCNT on the Si_3N_4 membrane.

the area and indeed observed a signal from an apparently individual semiconducting tube as described earlier. Assuming that the FWM signal originates from this SWCNT it is interesting to note that also in this case the signal is broadened with respect to the BBO reference data shown with a blue line in the figure. Similar analysis as for tube 1 yielded a dephasing time of 40−45 fs which is in line with the result obtained for tube 1. The strong signal from this tube allowed making further tests. In Figure 5a the spectrum of the FWM signal measured from the SWCNT (black line) is presented together with the corresponding spectrum measured from the BBO (blue line). The similarity of the spectra indicates that a correct FWM signal is detected. In addition, it was verified that the signal originates from a localized object by scanning the measurement beam over the tube with a piezo-positioner with a step size of 100 nm. The result is shown in Figure 5b indicating a cross section of ~800 nm which is approximately the size of the measurement beam according to the NA of the objective.

CONCLUSIONS

We have presented the first femtosecond FWM measurements of individual suspended SWCNTs. To verify the nature of the measured tubes, they were characterized by electron diffraction and Raman spectroscopy. This analysis confirmed that the tubes are individual and semiconducting and, moreover, their absolute structure was determined with the assignment of the chiral indices to 28,14 and 24,14. An approximate average electronic dephasing time of 40−45 fs was deter-

mined which is in a reasonable agreement with the existing literature values. The presented methodology opens the door to direct time-domain studies of excitonic and vibrational dynamics of individual SWCNTs.

MATERIALS AND METHODS

The samples were made on a 500 μm thick, double-side polished ⟨100⟩ Si wafer with a 200 nm thick dielectric layer of Si_3N_4 on both sides. First a 750 × 750 μm^2 opening in the bottom Si_3N_4 layer was made, using optical lithography followed by reactive ion etching at a pressure of 55 mTorr and 150 W power with a gas flow of 50 sccm of CHF_3 and 5 sccm of O_2. This was followed by wet etching through the Si wafer in 35% KOH at 97 °C, with an etch rate of ~180 μm/h. The etching process is anisotropic with an etching angle of 54.7°, resulting in a ~50 × 50 μm Si_3N_4 membrane window on the front side. A slit opening with the dimensions 2 × 40 μm was made in the Si_3N_4 membrane, using electron beam lithography followed by a second reactive ion etching. The bottom of the sample was then covered by a 25 nm thick layer of Pd preceded by a 5 nm thick sticking layer of Ti. The metal layer supports the membrane and can be used for gating purposes.

SWCNTs were grown across the membrane in a vertical CVD reactor. CO was used as the carbon source, Ni as the catalyst material, and CNT growth temperature was 740 °C. The SWCNT synthesis is described in more detail elsewhere.[23,24] The morphology and structure of the suspended carbon nanotubes were characterized in a Philips CM200-FEG transmission electron microscope (TEM), which is equipped with a Gatan 794 multiscan charge-coupled device (CCD) camera for digital data recording.

Raman measurements on the suspended tubes were performed with a home-built Raman spectrometer in a backscattering geometry. The setup is described in detail in ref 25. In short, 532 nm excitation wavelength with 2−4 mW power was used, focusing was performed with a microscope objective (Nikon 100×, 0.70 N.A.) and the backscattered light was collected with the same objective.

The FWM measurements were performed with an amplified femtosecond laser system. A schematic of the measurement setup is shown in Figure 6. Part of the 1 kHz output of the laser (Quantronix, Integra-3.5) was used to pump two home-built noncollinear optical amplifiers (NOPAs) to produce approximately 50 fs pump, Stokes and probe pulses for the experiment. The pump wavelength was chosen as 532 nm based on the Raman measurements that indicated resonance at this wavelength. Output of NOPA1 at 532 nm was used to produce pump and probe pulses. NOPA2 was tuned to 580 nm for Stokes pulse. This wavelength was chosen to be resonant with the G-band Raman transition with respect to the pump pulse. Well-collimated laser beams were focused to the sample using microscope objective (Olympus 50×, NA = 0.45) giving a spot with a diameter below 1 μm. Generated FWM signal was then collected in a back scattering geometry (epi-direction) using the same objective, and the signal was further separated from possible scattered light of the incoming beams by using long pass dichroic beamsplitter (LPDB) (511 BrightLine Dichroic Beamsplitter, Semrock) and a monochromator (Acton SP-150i equipped with 300 grooves/mm grating). The collection of the signal in epi-direction is advantageous for detection of weak signal in the presence of strong input pulses. FWM signal propagates to forward and backward directions when the measured object is much smaller than the wavelength of used light.[20] Signal was detected using a cooled photomultiplier tube (PMT) to reduce thermal noise.

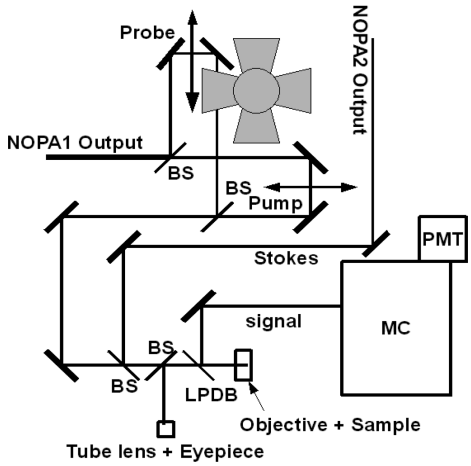

Figure 6. Optical arrangement for collinear FWM experiment. (BS = 50/50 beamsplitter, LPDB = long-pass dichroic beamsplitter, MC = monochromator, and PMT = photomultiplier tube).

For some measurements, the probe beam was chopped at 500 Hz and the signal was recorded using a lock-in-amplifier. Lock-in amplifier output was further averaged using Boxcar averager and digitized to the computer controlling optical delay lines and piezo-positioners (AttoCube Systems) which were used for sample movement. When aligning the beams to the sample, a tube lens and an eyepiece (10×) was installed on the signal line (see Figure 6) in order to visually pinpoint the beams to the right position.

All pulses were well collimated and aligned to collinear geometry. Beam sizes were adjusted to match clear aperture of the objective. Timing of the pulses was controlled using optical delay lines; pump−stokes delay was adjusted to zero while stokes−probe delay was scanned. Pulse energies of all three incoming pulses were adjusted to *ca.* 1 − 2 nJ/pulse (0.3−0.5 J/cm^2/pulse) at the sample position. Care was taken to ensure that no photodamage was induced during the signal collection. Using too high pulse energy could cause irreversible photodamage leading to decay and finally total loss of the signal. Typically 1000 pulses per data point were averaged to obtain reasonable S/N-ratio for the detected signal. The samples were aligned so that the polarization of the excitation beams was parallel to the nanotube axis.

Acknowledgment. This project was supported by the Academy of Finland (No. 117937, 118232, and 128445), the Finnish National Graduate School in Nanoscience (NGS-NANO), and by the Finnish TEKES GROCO Project (1298/31/08).

REFERENCES AND NOTES

1. Brus, L. Noble Metal Nanocrystals: Plasmon Electron Transfer Photochemistry and Single-Molecule Raman Spectroscopy. *Acc. Chem. Res.* **2008**, *41*, 1742–1749.
2. Dresselhaus, M. S.; Dresselhaus, G.; Jorio, A. Raman Spectroscopy of Carbon Nanotubes in 1997 and 2007. *J. Phys. Chem. C* **2007**, *111*, 17887–17893.
3. Bachilo, S. M.; Strano, M. S.; Kittrell, C.; Hauge, R. H.; Smalley, R. E.; Weisman, R. B. Structure-Assigned Optical Spectra of Single-Walled Carbon Nanotubes. *Science* **2002**, *298*, 2361–2366.
4. Reich, S.; Thomsen, C.; Maultzsch, J. *Carbon Nanotubes: Basic Concepts and Physical Properties*; Wiley-VCH: Weinheim, Germany, 2004.
5. Sfeir, M. Y.; Beetz, T.; Wang, F.; Huang, L.; Huang, X. M. H.; Huang, M.; Hone, J.; O'Brien, S.; Misewich, J. A.; Heinz, T. F.; *et al.* Optical Spectroscopy of Individual Single-Walled Carbon Nanotubes of Defined Chiral Structure. *Science* **2006**, *312*, 554–556.
6. Berciaud, S.; Voisin, C.; Yan, H.; Chandra, B.; Caldwell, R.; Shan, Y.; Brus, L. E.; Hone, J.; Heinz, T. F. Excitons and High-Order Optical Transitions in Individual Carbon Nanotubes: A Rayleigh Scattering Spectroscopy Study. *Phys. Rev. B* **2010**, *81*, 041414(R).

7. Seferyan, H.; Ye; Nasr, M. B.; Senekerimyan, V.; Zadoyan, R.; Collins, P.; Apkarian, V. A. Transient Grating Measurements of Excitonic Dynamics in Single-Walled Carbon Nanotubes: The Dark Excitonic Bottleneck. *Nano Lett.* **2006**, *6*, 1757–1760.
8. Kang, K.; Ozel, T.; Cahill, D. G.; Shim, M. Optical Phonon Lifetimes in Single-Walled Carbon Nanotubes by Time-Resolved Raman Scattering. *Nano Lett.* **2008**, *8*, 4642–4647.
9. Ikeda, K.; Uosaki, K. Coherent Phonon Dynamics in Single-Walled Carbon Nanotubes Studied by Time-Frequency Two-Dimensional Coherent Anti-Stokes Raman Scattering Spectroscopy. *Nano Lett.* **2009**, *9*, 1378–1381.
10. Zhu, Z.; Crochet, J.; Arnold, M. S.; Hersam, M. C.; Ulbricht, H.; Resasco, D.; Hertel, T. Pump−Probe Spectroscopy of Exciton Dynamics in (6,5) Carbon Nanotubes. *J. Phys. Chem. C* **2007**, *111*, 3831–3835.
11. Graham, M. W.; Ying-Zhong, M.; Fleming, G. R. Femtosecond Photon Echo Spectroscopy of Semiconducting Single-Walled Carbon Nanotubes. *Nano Lett.* **2008**, *8*, 3936–3941.
12. Kim, H.; Sheps, T.; Collins, P. G.; Potma, E. O. Nonlinear Optical Imaging of Individual Carbon Nanotubes With Four-Wave-Mixing Microscopy. *Nano Lett.* **2009**, *9*, 2991–2995.
13. Jiang, H.; Nasibulin, A. G.; Brown, D. P; Kauppinen, E. I. Unambiguous Atomic Structural Determination of Single-Walled Carbon Nanotubes by Electron Diffraction. *Carbon* **2007**, *45*, 662–667.
14. Jorio, A.; Pimenta, M. A.; Souza Filho, A. G.; Saito, R.; Dresselhaus, G.; Dresselhaus, M. S. Characterizing Carbon Nanotube Samples With Resonance Raman Scattering. *New J. Phys.* **2003**, *5*, 139.1139.17.
15. Araujo, P. T.; Maciel, I. O.; Pesce, P. B. C.; Pimenta, M. A.; Doorn, S. K.; Qian, H.; Hartschuh, A.; Steiner, M.; Grigorian, L.; Hata, K.; *et al*. Nature of the Constant Factor in the Relation Between Radial Breathing Mode Frequency and Tube Diameter for Single-Wall Carbon Nanotubes. *Phys. Rev. B* **2008**, *77*, 241403(R).
16. Michel, T.; Paillet, M.; Nakabayashi, D.; Picher, M.; Jourdain, V.; Meyer, J. C.; Zahab, A. A.; Sauvajol, J.-L. Indexing of Individual Single-Walled Carbon Nanotubes from Raman Spectroscopy. *Phys. Rev. B* **2009**, *80*, 245416.
17. Meyer, J. C.; Paillet, M.; Michel, T.; Moréac, A.; Neumann, A.; Duesberg, G. S.; Roth, S.; Sauvajol, J.-L. Raman Modes of Index-Identified Freestanding Single-Walled Carbon Nanotubes. *Phys. Rev. Lett.* **2005**, *95*, 217401.
18. Débarre, A.; Kobylko, M.; Bonnot, A. M.; Richard, A.; Popov, V. N.; Henrard, L.; Kociak, M. Electronic and Mechanical Coupling of Carbon Nanotubes: A Tunable Resonant Raman Study of Systems with Known Structures. *Phys. Rev. Lett.* **2008**, *101*, 197403.
19. Mukamel, S. *Principles of Nonlinear Spectroscopy*; Oxford University Press: New York, 1999.
20. Evans, C. L.; Xie, X. S. Coherent anti-Stokes Raman Scattering Microscopy: Chemical Imaging for Biology and Medicine. *Annu. Rev. Anal. Chem.* **2008**, *1*, 883–909.
21. Maultzsch, J.; Telg, H.; Reich, S.; Thomsen, C. Radial Breathing Mode of Single-Walled Carbon Nanotubes: Optical Transition Energies and Chiral-Index Assignment. *Phys. Rev. B* **2005**, *72*, 205438.
22. Araujo, P. T.; Doorn, S. K.; Kilina, S.; Tretiak, S.; Einarsson, E.; Maruyama, S.; Chacham, H.; Pimenta, M. A.; Jorio, A. Third and Fourth Optical Transitions in Semiconducting Carbon Nanotubes. *Phys. Rev. Lett.* **2007**, *98*, 067401.
23. Mudimela, P. R.; Nasibulin, A. G.; Jiang, H.; Susi, T.; Chassaing, D.; Kauppinen, E. I. Incremental Variation in the Number of Carbon Nanotube Walls with Growth Temperature. *J. Phys. Chem. C* **2009**, *113*, 2212–2218.
24. Queipo, P.; Nasibulin, A. G.; Gonzalez, D.; Tapper, U.; Jiang, H.; Tsuneta, T.; Grigoras, K.; Duenas, J. A.; Kauppinen, E. I. Novel Catalyst Particle Production Method for CVD Growth of Single- and Double-Walled Carbon Nanotubes. *Carbon* **2006**, *44*, 1604–1608.
25. Rintala, J.; Herranen, O.; Johansson, A.; Ahlskog, M.; Pettersson, M. Raman Spectroscopy and Low-Temperature Transport Measurements of Individual Single-Walled Carbon Nanotubes with Varying Thickness. *J. Phys. Chem. C* **2009**, *113*, 15398–15404.